

Recombinative desorption of H₂ on Si(100)-(2×1) and Si(111)-(7×7): Comparison of internal state distributions

Stacey F. Shane,^{a)} Kurt W. Kolasinski,^{b)} and Richard N. Zare
Department of Chemistry, Stanford University, Stanford, California 94305

(Received 5 March 1992; accepted 3 April 1992)

The dynamics of recombinative hydrogen desorption from the Si(100)-(2×1) and Si(111)-(7×7) surfaces have been compared using (2 + 1) resonance-enhanced multiphoton ionization to probe the desorbed H₂. After dosing the surface with disilane (Si₂H₆), we performed temperature programmed desorption in a quantum-state-specific manner. The rovibrational-state distributions of H₂ desorbed from both Si(100)-(2×1) and Si(111)-(7×7) are found to be *the same* within experimental accuracy. The rotational distribution is non-Boltzmann and has an average energy significantly lower than kT_s , where T_s is the surface temperature. In contrast, superthermal energy is observed in the vibrational degree of freedom, and the $v = 1$ to $v = 0$ population ratio is approximately 20 times higher than that predicted by Boltzmann statistics. Our results imply that the details of the recombinative desorption process that affect the product state distribution are remarkably insensitive to the structural differences between the surfaces. We suggest that the transition-state geometry is similar on both surfaces and propose a model for hydrogen recombinative desorption localized at a single silicon atom.

I. INTRODUCTION

A fundamental example of a heterogeneous chemical reaction is the recombinative desorption of two atoms from a well-defined surface. In a simple picture, recombinative desorption involves the scission of two atom-surface bonds and the formation of a single new atom-atom bond to produce the molecular product. Such an elementary description of the process may underestimate the role of the surface, however. Effects such as surface reconstruction, modification of the local electronic structure, or even the formation and breaking of bonds between surface atoms may influence both the energetics and the dynamics of the reaction. Bonding in the solid and the adsorbate (which in this case is dissociated) is weakened as a result of adsorbate-surface bonding,¹ although assessing such an effect in a metal can be difficult, the weakening or breaking of substrate bonds often is more easily identified for a covalent solid.

In a covalent solid, bonding is produced by overlap of the highly directional orbitals of hybridized atoms. The reactivity of many covalent surfaces is strongly controlled by the unsatisfied hybrid bonding orbitals, or dangling bonds (dbs), that remain upon truncating the bulk. Such surfaces are driven to minimize their total free energy through a trade-off between energy gained by local bond formation (eliminating dangling bonds) with energy lost because of resulting bond strain.^{2,3} This trade-off often leads to complex surface reconstructions.

In the present work we compare the recombinative desorption of hydrogen from Si(100) and Si(111). Both surfaces undergo extensive reconstructions that are strongly coupled to the presence of adsorbed hydrogen. The resulting

surfaces are markedly different. The Si(100) surface reconstructs to a (2×1) structure that consists of pairs of silicon atoms in adjacent rows that have bonded to each other, thereby reducing the number of dangling bonds from two per surface atom to one. Si(111) reconstructs into a complex (7×7) structure with 19 dangling bonds per unit cell (reduced from 49) that reside on silicon adatom (12 dbs), rest-atom (6), and corner-hole (1) sites. Figure 1 illustrates the Si(100)-(2×1) and Si(111)-(7×7) surfaces. The Si(111)-(7×7) surface has a significantly lower density of surface dangling bonds than the Si(100)-(2×1) surface (34 Å²/db vs 15 Å²/db).

The behavior of hydrogen on silicon, and of adsorbates on covalent surfaces in general, is strongly controlled by the dangling bond orbitals⁴ and the strained bonds of the reconstructed surface. Adsorption of atomic hydrogen on both Si(100)-(2×1) and Si(111)-(7×7) is well studied.^{3,5-10} Hydrogen initially saturates the dangling bonds by producing monohydride groups (SiH), leaving the reconstruction relatively intact. Upon further exposure, however, hydrogen (reversibly) attacks the most highly strained Si-Si bonds on either surface. On the Si(100)-(2×1) surface, saturation of the monohydride phase leads to a relaxation of some of the bond strain in the near surface region, although the (2×1) periodicity is maintained.^{7,11} At higher coverages, however, the Si-Si dimer bond is attacked by hydrogen, forming dihydride (SiH₂) species. Based on scanning tunneling microscopy (STM) studies, Boland³ has reported that the Si(111)-(7×7) reconstruction is severely modified, even at much lower coverages of hydrogen. Although the (7×7) unit cell remains, the STM results reveal the formation of silicon adatom islands. Hydrogen in the monohydride form is bound on this surface to the restlayer atoms and the island adatoms,³ resulting in a nearly bulklike (1×1) periodicity within the (7×7) triangular subunits. The removal of hydrogen from this surface regenerates the (7×7) structure pictured in Fig. 1(b), a result that implies that significant motion of surface

^{a)} Present address: AT&T Bell Laboratories, 600 Mountain Avenue, Murray Hill, New Jersey 07974.

^{b)} Present address: Fritz-Haber-Institut der Max-Planck-Gesellschaft, Faradayweg 4-6, D-1000 Berlin 33, Germany.

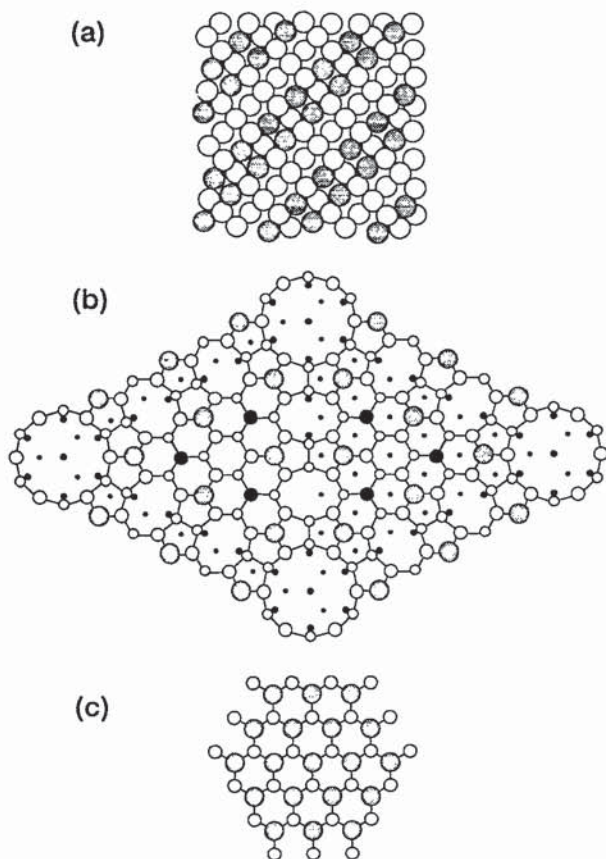


FIG. 1. A schematic representation of the silicon surfaces. (a) Top view of the Si(100)-(2 \times 1) surface. (b) Top view of the dimer-atom-stacking fault model of the Si(111)-(7 \times 7) reconstruction by Takayanagi *et al.* (Ref. 85). Atoms at increasing depth are represented by circles of decreasing diameter in this representation. (c) Top view of an unreconstructed Si(111) surface. The silicon atoms with dangling bonds are shaded on each surface; in (b) the largest solid circles also represent atoms with dangling bonds. These shaded and solid atoms are the sites at which the monohydride most likely binds.

atoms and changes in surface bonding accompany desorption.

In light of these significant structural differences, it is at first surprising that the thermal desorption properties of the hydride species should be similar on the Si(100)-(2 \times 1) and Si(111)-(7 \times 7) surfaces. Temperature-programmed desorption (TPD) spectra of H₂ from *both* the Si(100)-(2 \times 1) (Refs. 12–14) and Si(111)-(7 \times 7) (Refs. 5, 13, and 15) surfaces are characterized by two peaks: a higher temperature β_1 peak near 780 K that arises from desorption from the monohydride, and a lower temperature β_2 peak at \sim 670 K that correlates with desorption from the dihydride (and trihydride, SiH₃).

Although the TPD spectra indicate that desorption occurs at similar rates from the two surfaces, recent experiments of monohydride desorption using laser-induced thermal desorption (LITD) have revealed that the kinetic order differs.^{13,16} At moderate to high coverages, the Si(111)-(7 \times 7) surface is characterized by second-order H₂ desorption kinetics with reported activation barriers and preexponential factors that range from 59–63 kcal/mol and 0.05–231 cm²s⁻¹ respectively.^{5,13,15} In contrast, desorption from the

Si(100)-(2 \times 1) surface follows first-order kinetics.^{13,16,17} Markedly different values of kinetic parameters have been reported for this first-order rate: Sinniah *et al.*¹⁶ measure an activation energy, E_a , of 45 ± 2 kcal/mol and a preexponential factor of $2.2 \pm 0.3 \times 10^{11}$ s⁻¹ whereas both Wise *et al.*¹³ and Höfer, Li, and Heinz¹⁷ report $E_a = 58 \pm 2$ kcal/mol with prefactors of $5.5 \pm 0.5 \times 10^{15}$ s⁻¹ and $\sim 2 \times 10^{15}$ s⁻¹, respectively. We note that first-order kinetics are not in accord with a conventional random hopping picture for a bimolecular recombination reaction.^{18,19}

Recent measurements by Heinz and co-workers^{17,20} using optical second harmonic generation have indicated that at low coverages ($\Theta < 0.1$ –0.2), the reaction order departs from that reported at higher coverages on both the Si(100)-(2 \times 1) and Si(111)-(7 \times 7) surfaces. On Si(100)-(2 \times 1), the reaction order increases to greater than first order as the coverage is decreased,¹⁷ whereas on Si(111)-(7 \times 7), the reaction order decreases from quadratic to an intermediate reaction order of $m = 1.5 \pm 0.2$.²⁰ Studies on the diffusion of atomic hydrogen on Si(111)-(7 \times 7) by Reider, Höfer, and Heinz²¹ have shown that while the frequency factor compares with that on metals, the barrier for diffusion is much larger. These researchers measured the diffusion barrier to be $E_{\text{diff}} = 1.5 \pm 0.2$ eV, which is approximately 50% of the estimated binding energy.

In this report, we investigate the role of surface structure²² on the *dynamics* of recombinative hydrogen desorption from silicon. We present the results of state-specific studies of H₂ recombinative desorption from the monohydride species on the (100)-(2 \times 1) and (111)-(7 \times 7) surfaces. Dynamical studies of the dihydride desorption will be reported elsewhere.²³ The surface monohydride species in this study were produced by adsorption of disilane. Because of the extremely low reactivity of molecular hydrogen with the Si(100) and Si(111) surfaces,^{5,24–27} both atomic hydrogen and disilane (Si₂H₆), which have high sticking probabilities at room temperature, are commonly used as sources of surface hydrogen.²⁸ Several studies have shown that the source of hydrogen has little effect on the properties of the hydride species formed on both the Si(100)-(2 \times 1) and the Si(111)-(7 \times 7) surfaces, although the stability of the mono-, di-, and trihydride depends strongly on coverage and temperature.^{4,29–31} Furthermore, we have previously compared the rovibrational distribution of H₂ desorbed from Si(100)-(2 \times 1) after both disilane and atomic hydrogen adsorption and found that the source of surface hydrogen has no effect on the internal state distribution of the desorbed H₂.³²

The low sticking probability of H₂ is usually attributed to the presence of a significant energetic barrier to dissociative adsorption,³³ although orientational restrictions may also play a role. By detailed balance, a barrier in the adsorption channel has implications for the reverse process of desorption, namely, superthermal energy may be released to the desorbing H₂. In our previous studies of H₂/Si(100)-(2 \times 1),³⁴ we observed that H₂ does desorb with superthermal vibrational energy, with a $v = 1$ to $v = 0$ population ratio approximately 20 times higher than that predicted by Boltzmann statistics at the surface temperature, $T_s = 800$ K.

The rotational distribution is also non-Boltzmann, although in contrast to the vibrational distribution, the average rotational energy is significantly lower than kT_s . In the present study, we compare the rovibrational distribution of H₂ recombinationally desorbed from the Si(111)-(7×7) surface with that from Si(100)-(2×1). The results show marked similarities in the rovibrational distributions obtained from the two surfaces. The nature of the silicon surface, with its highly directional bonding and large diffusion barrier, leads us to describe silicon in a local model. Based upon these results, a model is presented for recombinationally desorption localized at a single silicon atom.

II. EXPERIMENTAL

A detailed description of the experimental technique may be found elsewhere.³⁴ The basic measurement is quantum-state-resolved temperature-programmed desorption. A monohydride-covered silicon surface is prepared by adsorbing a saturation dose of disilane, Si₂H₆. During the subsequent TPD, the H₂ desorption flux is intersected by a pulsed laser beam and ionized via (2 + 1) resonance-enhanced multiphoton ionization (REMPI). At a set laser frequency, we follow the intensity of ions resulting from a particular H₂(*v*,*J*) state as a function of crystal temperature. The quantum-resolved TPD spectra are then reduced to relative rovibrational populations.

A. Apparatus and reagents

A diagram of the experimental apparatus is shown in Fig. 2. The experiments are performed in an ultrahigh vacuum (UHV) chamber with a base pressure of 4×10^{-10} torr. Attached to the main UHV chamber is a source chamber that contains a pulsed nozzle and a skimmer. The nozzle and skimmer are invaginated into the main chamber, which allows the pulsed nozzle to be only 10 cm from the crystal to obtain a high beam flux. Both chambers are pumped by turbomolecular pumps (Balzers). The crystal is mounted on a manipulator in the main chamber, which also contains low-energy electron diffraction (LEED) with a retarding field analyzer (RFA) and Auger electron spectroscopy (AES) to monitor surface order and cleanliness.

Both the Si(111) and Si(100) samples used in these experiments were cut from 3 in. wafers of highly As-doped

(0.002%) *n*-type silicon (oriented to within 0.5°) with a resistivity of 0.005 Ω cm (Virginia Semiconductor). The 0.5 mm thick, 10×13 mm rectangular samples were tension mounted in a niobium holder. A chromel-alumel thermocouple was placed in a 0.8 mm hole drilled into the crystal near the top and secured by high-temperature ceramic adhesives (Aremco). Additional thermocouples were placed underneath the crystal. The sample was resistively heated by applying current directly to the crystal and cooled by liquid nitrogen. A feedback circuit controlled the temperature.

The Si(111) and Si(100) samples were initially degreased in methanol and acetone then annealed at ~900 K for 12–48 h under vacuum. The Si(100)-(2×1) surface was prepared by flashing the sample to 1200 K to remove the native oxide. After slowly cooling, the crystal exhibited a sharp (2×1) LEED pattern, although generally some residual carbon contamination was detectable with AES.

Best results were obtained for the Si(111) surface by a modified preparation. After being annealed at 900 K, the sample was heated just enough to remove the native oxide (1200 K), just as for the Si(100) sample. This procedure, however, led to a sample that exhibited a (1×1) LEED pattern. Following Jansson and Uram,⁸ we proceeded to grow Si onto this surface by applying a beam of disilane for 10 min while the surface was held at 900 K. The resulting surface exhibited a sharp (7×7) LEED pattern. Some experiments were also performed on Si(111) samples that showed a (1×1) LEED pattern; no difference in the internal state distribution was observed.

Both the Si(100)-(2×1) and Si(111)-(7×7) surfaces were maintained by passivating the samples with an adsorbed hydrogen layer between experiments. After disilane experiments were run on a sample for several weeks, the LEED pattern began to lose its sharpness, and the samples were replaced. The Si(111)-(7×7) surface was observed by LEED measurements to deteriorate more quickly than the Si(100)-(2×1) surface. A total of six Si(100) and four Si(111) crystals were used in these experiments.

Disilane (Alphagaz, 99.8%) was used without additional purification. Neat disilane was used behind the pulsed nozzle (2 ms/pulse at 10 Hz), which produced a high enough flux to saturate the surface within 30 s. Both the Si(100)-(2×1) and Si(111)-(7×7) surfaces were dosed to saturation before each temperature-programmed desorption. A few comparative studies were made using atomic hydrogen as the dosant. The atomic hydrogen was produced by a hot tungsten filament situated a few centimeters from the surface in a background of H₂ gas.

B. H₂ detection scheme

Hydrogen is detected by (2 + 1) REMPI through the *E*, *F*, ¹Σ_g⁺ state. The spectroscopy of this transition is well characterized, and Rinnen *et al.*³⁵ have determined (*v*,*J*)-dependent correction factors under saturation conditions similar to ours, allowing reduction of ion signals into relative populations.

Probing the ground and first vibrationally excited states of H₂ requires tunable ultraviolet radiation in the wavelength range of 200 to 215 nm. The laser system consists of a

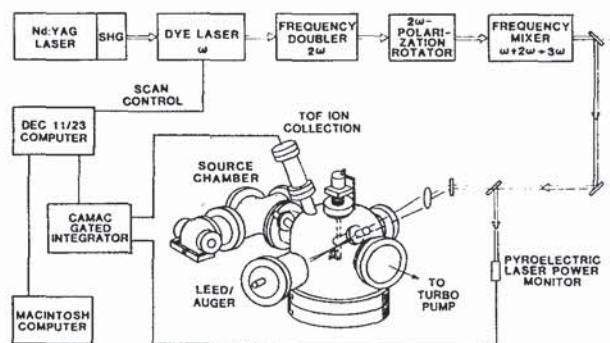


FIG. 2. Schematic diagram of the experimental apparatus.

pulsed Nd:YAG pumped dye laser (Quantel) and frequency doubling and mixing stages (Inrad). With this setup, 80–100 mJ of light at 600–645 nm is converted to 1–3 mJ of 200–215 nm radiation, which is sufficient to saturate both the excitation and ionization steps. This saturation is verified by an experimentally measured power dependence of 1.5, which agrees with the expected $\frac{3}{2}$ power law for a saturated multiphoton process.³⁶ The beam is directed into the vacuum chamber by dichroic mirrors (Virgo Optics), which also act to separate the tripled frequency from the residual fundamental and doubled frequencies. The light is focused into the chamber through a quartz window by a 350 mm focal length lens. The beam passes a few millimeters above the crystal surface and is subsequently blocked by a beam stop inside the chamber. A back reflection from the chamber window is sent into a pyroelectric detector (Molelectron) for power normalization.

The REMPI-produced H₂⁺ ions are mass-selectively detected by a time-of-flight (TOF) mass spectrometer situated above the crystal, as illustrated in Fig. 2. Ions are extracted into the TOF tube and detected by a two-stage microchannel plate chevron detector (Galileo). The output of the microchannel detector is collected by a CAMAC-crate-mounted gated integrator (LeCroy) and sent to a minicomputer (DEC PDP-11/23) for analysis. The ion signal is corrected for power variations on a shot-to-shot basis using the experimentally observed power dependence of 1.5.

We note that with the present experimental geometry, we effectively integrate over a large range of desorption angles, although the detection is slightly biased to desorption flux in the direction normal to the surface. Furthermore, the current detection scheme is insensitive to alignment effects in the desorbed H₂. Monopole (rank zero tensor) terms dominate a two-photon Σ - Σ transition probed with linearly polarized light.³⁷ The domination of the monopole term is the cause of the strong enhancement in Q -branch intensity over S and O branches and of the insensitivity to alignment, because a monopole is isotropic.³⁸

III. RESULTS

Figure 3 displays a typical thermal desorption spectrum of H₂($v=0, J=1$). The data were obtained by desorption of H₂ from Si(100)-(2×1) following a saturation dose of disilane. The crystal is heated at 10 K/s, and the power-corrected ion signal is followed in *time*, which is related linearly to surface temperature. We obtain similar desorption spectra for each (v, J)-quantum level that is sufficiently populated for detection.

To generate a population distribution, the power-corrected ion signal for each rovibrational state is integrated as a function of time, then corrected for the background contribution, as described previously.³⁴ The background-subtracted signals are converted to relative population by applying the (v, J)-dependent correction factors determined by Rinne *et al.*³⁵

Figure 4 displays the resulting rotational distributions in the form of a Boltzmann plot, in which the natural logarithm of the population divided by the rotational degeneracy ($2J+1$) and the nuclear spin degeneracy (g_N) is plotted

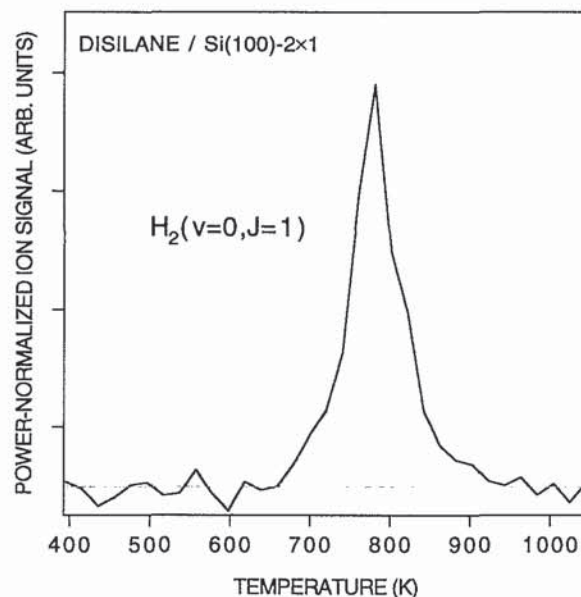


FIG. 3. Quantum-resolved thermal desorption spectrum for H₂($v=0, J=1$) desorbed from Si(100)-(2×1) after a saturation dose of Si₂H₆. The surface temperature during adsorption was 400 K, and the heating rate was 10 K/s.

versus rotational energy (E_J). The plot includes both H₂($v=0$) and H₂($v=1$) desorbed from the Si(100)-(2×1) and Si(111)-(7×7) surfaces. The relative positions of the $v=0$ and the $v=1$ rotational distributions accurately

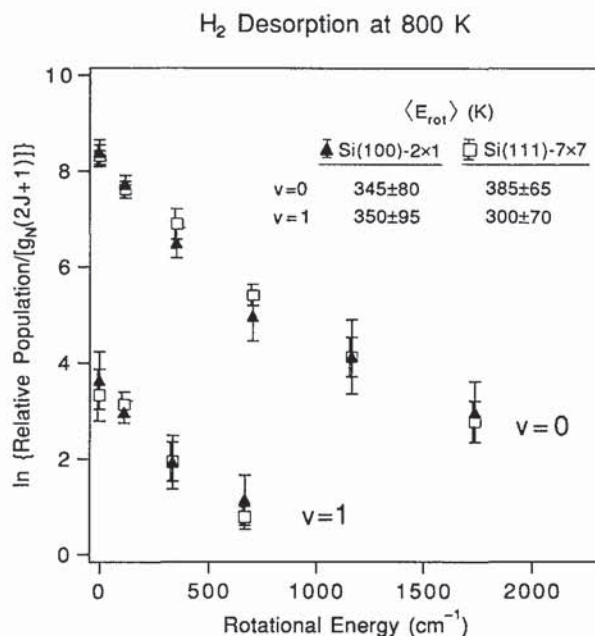


FIG. 4. Boltzmann plot of H₂ thermally desorbed from the Si(100)-(2×1) and Si(111)-(7×7) surfaces. The rotational distributions are shown for both the $v=0$ and $v=1$ vibrational states. The relative positions of the H₂($v=0$) and the H₂($v=1$) rotational distributions accurately represent the measured H₂($v=0$) to H₂($v=1$) population ratio. All data shown are for disilane adsorption, except for the H₂($v=1$) data from Si(111)-(7×7), which, because of small signal levels, were collected after dosing the sample with atomic hydrogen. As discussed in the text, the hydrogen distributions are not affected by the source of surface hydrogen.

represent the measured H₂(*v* = 0) to H₂(*v* = 1) population ratio.

Some of the early experiments on the Si(111) surface were performed on surfaces that did not clearly exhibit the LEED spots of the (7×7) reconstruction, although the level of carbon contamination measured by AES appeared similar to that of other samples. The structural makeup of this surface is unknown, but studies on laser-annealed (1×1) silicon surfaces have indicated that the local structure may have some similarities with the (7×7) surface.^{39,40} In any case, no systematic difference in the rovibrational distribution was observed between data taken on these crystals and data taken on crystals that did exhibit sharp (7×7) LEED patterns. We have used the combined data in our analysis.

Examination of Fig. 4 shows that the rovibrational distribution of desorbed H₂ is the same from both the Si(100)-(2×1) and Si(111)-(7×7) surfaces within the experimental accuracy. Figure 5 shows the H₂(*v* = 0) and H₂(*v* = 1) distributions from the Si(100)-(2×1) surface only, along with a dashed line that corresponds to a normalized Boltzmann distribution at *T*_{rot} = *T*_s = 800 K. Comparison of the H₂(*v* = 0)/Si(100)-(2×1) rotational distribution with the 800 K line reveals that the distributions are non-Boltzmann and the average rotational energy is lower than *kT*_s. We can quantify the rotational distribution by the average rotational energy, $\langle E_{\text{rot}} \rangle$, where

$$\langle E_{\text{rot}} \rangle (v) = \frac{\sum_J N_{vJ} E_J}{\sum_J N_{vJ}},$$

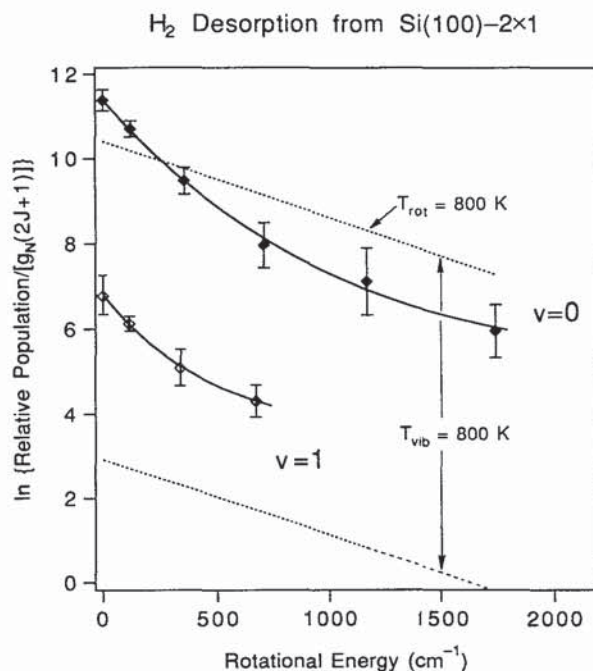


FIG. 5. Comparison of the measured rovibrational distribution of H₂ desorbed from Si(100)-(2×1) with a thermal distribution at the surface temperature, *T*_s = 800 K, shown on a Boltzmann plot. The experimental data are shown with markers; the solid curves through the data are provided to aid the eye. The top dashed line represents an 800 K rotational distribution, and the position of the bottom dashed line represents the relative population in *v* = 1 at 800 K.

where *N*_{*vJ*} is the relative population in the level (*v*, *J*) and *E*_{*J*} is the rotational energy of that level relative to *J* = 0. We find that $\langle E_{\text{rot}} \rangle (v = 0)/k$ is 385 ± 65 K and 345 ± 80 K for Si(111)-(7×7) and Si(100)-(2×1), respectively. For *v* = 1, $\langle E_{\text{rot}} \rangle/k$ is 300 ± 70 K (Ref. 41) for Si(111)-(7×7) and 350 ± 95 K for Si(100)-(2×1). Within experimental uncertainty, the average rotational energies for H₂(*v* = 0) and H₂(*v* = 1) from the Si(111)-(7×7) surface are identical to those from the Si(100)-(2×1) surface. Furthermore, they do not differ significantly between the *v* = 0 and *v* = 1 states. Compared with the mean rotational energy of a Boltzmann distribution at 800 K ($\langle E_{\text{rot}} \rangle/k = 783$ K for H₂), the average rotational energies for H₂ desorbed from Si are much lower.

In contrast, the vibrational distribution is superthermal. The lower dashed line in Fig. 5 represents the population of H₂(*v* = 1) that would be expected for an 800 K distribution relative to the actual H₂(*v* = 0) distribution, according to $N_{v=1}/N_{v=0} = \exp(-[E(v=1) - E(v=0)]/kT_s)$. The H₂(*v* = 1) population for the desorbed hydrogen is clearly higher. The population in H₂(*v* = 1) is enhanced over a thermal distribution by a factor of 25 ± 10 for the Si(100)-(2×1) surface, and 20 ± 10 for the Si(111)-(7×7) surface, where the thermal $N_{v=1}/N_{v=0}$ absolute population ratio is 0.000 465 at 780 K. Attempts to detect H₂ in *v* = 2 were unsuccessful.

In the aforementioned analysis, we have assumed the measured quantity corresponds to desorption flux, which is the correct parameter to describe surface desorption. Based upon estimates of the focal parameters of the laser and the velocity of desorbed H₂, however, we calculate that our detector is neither a pure flux nor a number density detector, but rather a combination of both. Strictly speaking, the data are related to flux by some function of the velocity, which may be dependent on both *v* and *J*. Velocity information of H₂ desorbed from Si is unknown; although the velocity is likely to be independent of rotational state as observed for H₂/Pd,⁴² it could be correlated with vibrational state. Rough calculations indicate that even if the mean translational energies differ by one quantum of vibration (i.e., the total energy is the same for *v* = 1 and *v* = 0), our results would be unaffected within experimental error. Furthermore, the observed trends of low rotational energy, vibrational excitation, and the same distribution for both surfaces should be largely independent of such velocity effects.

Relating the measured product distribution to the dynamics of a specific reaction requires confirmation that the experiment actually measures the direct product, i.e., secondary processes that might modify the nascent distribution must be considered. We have addressed in detail the question of rotational state changing events occurring after formation of H₂ (Ref. 34), and conclude that such processes are unimportant.

Finally, to rule out any influence of the silicon adatoms present on the surface after adsorption of disilane, we performed some experiments with adsorption of atomic hydrogen. The potential effect of silicon adatoms is an important consideration, because if the desorption process were dominated by the deposited silicon, the influence of the innate

structural differences of the Si(111)-(7×7) and Si(100)-(2×1) surfaces on the reaction might be obscured. The structures and properties of H-atom- and disilane-dosed Si surfaces have been the subject of extensive investigation.^{3,4,8,9,28,29,31,43–49} In previous publications,^{32,34,50} we have reviewed the pertinent details of this body of work and have concluded that significant differences are not expected in the temperature range of interest to this study. Furthermore, we have explicitly tested this premise by measuring the rovibrational state distributions of hydrogen desorbed from the Si(100)-(2×1) (Ref. 32) and Si(111)-(7×7) surfaces. We have observed no difference in the rovibrational state distribution that can be correlated to the source of adsorbed hydrides.

IV. DISCUSSION

In the present study, we have determined the internal state distribution of molecular hydrogen recombinatively desorbed from two faces of single-crystal silicon. We observe significant rotational cooling in the product H₂, with an average rotational energy less than half of that predicted for a Boltzmann distribution at the surface temperature of approximately 780 K. In contrast, we find excess energy in the vibrational degree of freedom; the population in H₂($\nu = 1$) is enhanced by more than a factor of 20 over a 780 K thermal distribution. Based on isotopic studies,³⁴ we believe that our measured internal state distributions represent the nascent energy distribution of the H₂ product, unperturbed by subsequent energy (rotational or vibrational) exchange. We are then led to interpret the measured distributions.

Recombinative desorption on a covalent surface such as silicon is perhaps best thought of in a local model. The interaction of hydrogen with the surface is strong and highly directional, and diffusion is not facile, in contrast to the behavior of hydrogen on many metal surfaces. In the limit of very little surface interaction, where the surface acts primarily as a sink or source of energy and momentum, the surface reaction is somewhat analogous to a gas-phase bimolecular recombination reaction with a “third body.” Such a model may be appropriate for some recombination reactions on metal surfaces. For the case of hydrogen on silicon, however, the interaction with the surface is expected to be strongly localized and the lowest energy process for recombinative desorption probably involves a concerted breaking of H–Si bonds and formation of a H–H bond. Such a mechanism is more closely related to gas-phase molecular elimination, which may be a useful starting point for a model.

The observation of a nonthermal energy distribution suggests the importance of dynamical constraints in the desorption process. From the low average rotational energy of the desorbed H₂, we conclude that little torque is applied to molecular hydrogen during formation, i.e., the angular momentum associated with the reaction complex is small. Following concepts developed for molecular dynamics,^{51–54} we propose that the reaction proceeds through a transition state that is symmetrically constrained with respect to the corrugation in the potential-energy surface. Furthermore, we propose that the transition state is characterized by a H–H separation larger than that of the free H₂ molecule, consistent

with the production of a vibrationally excited product.

Our measured internal state distributions are in good agreement with a very recent calculation by Sheng and Zhang on the Si(100)-(2×1) surface.⁵⁵ Using a simple theoretical model in which desorption of H₂ results from a bound-free transition from initially bound H–Si states to a final continuum H₂ plus Si state, Sheng and Zhang have predicted H₂ rotational and vibrational state distributions very close to what we measure. Their model predicts that H₂ will desorb rotationally cold; the calculated average rotational energy agrees with the measured value for H₂($\nu = 1$) within experimental error, and is in qualitative agreement for H₂($\nu = 0$). Furthermore, the calculated vibrational enhancement over a thermal distribution at the surface temperature is 33.5, compared to the experimental value of 25 ± 10 on Si(100)-(2×1). The model of Sheng and Zhang predicts, however, that the internal state distribution will be sensitive to surface structure, in contrast to the experimental observation. In Sec. IV A, we draw upon the Si(100)-(2×1)/Si(111)-(7×7) comparative study to develop a more detailed model of recombinative hydrogen desorption.

A. Comparison of Si(100)-(2×1) and Si(111)-(7×7): Implications for a transition state localized at a single silicon atom

The most striking result of this study is the observation that the rotational and vibrational distribution of H₂ is, within the accuracy of the experiment, the same for both the Si(111)-(7×7) surface and the Si(100)-(2×1) surface. This similarity implies that the details of the recombinative desorption process that affect the product state distribution are remarkably insensitive to what appear to be significant differences in surface structure.

The surface geometry varies significantly with the crystallographic orientation of silicon, particularly when surface reconstructions are considered. Recall the pictorial representation of the Si(111)-(7×7) and Si(100)-(2×1) surfaces in Fig. 1. Although the exact surface structure and binding sites of hydrogen after adsorption of disilane are not known, we use the binding sites for atomic hydrogen adsorption as a guide for comparison. The silicon sites at which H atoms are believed to bind at low coverage in the monohydride form are indicated by shading. At higher doses of atomic hydrogen on the Si(111)-(7×7) surface, the adatoms form islands resulting in monohydride species bound primarily to the rest-layer atoms and to the island adatoms.³ Locally, the silicon structures within the (7×7) triangular subunits in this configuration have roughly (1×1) periodicity,⁵⁶ like that of the ideal Si(111) surface [Fig. 1(c)]. The H–H separation between adjacent sites (i.e., the smallest separations) on Si(100)-(2×1) is smaller than that on Si(111), whether we assume the (7×7) or the (1×1) structure.

The electronic structure also differs between the two surfaces. On the clean Si(100)-(2×1) surface, there is a π -bondinglike interaction between the electrons of the dangling bond orbitals on the dimer atoms.⁵⁷ Estimates for the strength of this interaction vary; reported values include 1–2 kcal/mol,^{58,59} 5–12 kcal/mol,^{17,60} and even up to 19

kcal/mol.⁴⁷ The π -bonding interaction is lost by adsorption of a H atom onto one of the atoms of the dimer. Such an effect is not known to exist on the Si(111)-(7 \times 7) surface. The presence of the π bond on the Si(100)-(2 \times 1) surface has been postulated to play an important role in the observed first-order rate law for hydrogen recombinative desorption on this surface.^{34,47,61} Recall that the rate law for desorption from Si(111)-(7 \times 7) is, in contrast, second order at moderate-to-high coverage.

The fact that different reaction orders are observed on the two surfaces indicates that the surface structure measurably affects the recombinative desorption of H₂. In contrast to the kinetic order and despite obvious structural differences, the product internal state distribution is the same from the Si(111)-(7 \times 7) and Si(100)-(2 \times 1) surface. Both the rotational- and vibrational-state distributions should reflect the dynamics of desorption and be sensitive to the transition-state geometry. Clearly, any model of recombinative hydrogen desorption from silicon must include a mechanism that is relatively insensitive to surface structure.

One possibility is the limiting case of a delocalized reaction that occurs far from the plane of the surface, whereby the reactants do not feel the surface corrugation. Such a model was proposed by Kubiak *et al.*⁶² to explain their measurement of the same rotational distribution (albeit different vibrational distributions) of H₂ desorbed from Cu(111) and Cu(110). We do not believe such a delocalized process is likely on the covalently bonded silicon surface. As discussed earlier, the interaction of hydrogen with the surface is localized, and there is a large diffusion barrier, in contrast to the behavior of hydrogen on copper. We are led then to the other possible extreme, namely, that the reaction is highly localized.

Because of the localized nature of bonding on the Si surface, the desorption mechanism probably involves very few silicon atoms. Furthermore, whatever the specific active site is, it must be present on both the Si(111)-(7 \times 7) and Si(100)-(2 \times 1) surfaces. One possibility is a defect site. Recent scanning tunneling microscopy studies indicate that even on carefully prepared silicon surfaces, the defect density is quite large.^{63,64} A defect model would have to include different concentrations of the defect site on the two surfaces and/or different binding energies to account for the different kinetic order observed.⁶⁵ If desorption occurred only at defects, the quality of the surface (i.e., defect density) should influence the desorption rate. For a reaction limited by availability of defect sites, a variation in defect density would be expected to appear in the rate expression as a change in preexponential factor. Calculations using the reported kinetic parameters^{13,16} indicate that a factor of 10 reduction in the preexponential factor would cause an increase in the temperature-programmed desorption peak temperature of as high as 80 K.⁶⁶ Such an effect has not been reported, however; in fact, studies on porous silicon⁶⁷ showed similar hydrogen desorption rates to that of the Si(100)-(2 \times 1) and Si(111)-(7 \times 7) single-crystal surfaces. Furthermore, H₂ desorption rates during epitaxial growth of Si (via adsorption of disilane), a process that may introduce defects, are also the same. We consider the defect mechanism implausi-

ble, although the possibility cannot be excluded.

The silicon dimer may play an important role in the recombinative desorption of hydrogen from the Si(100)-(2 \times 1) surface.^{13,34,47,61} A mechanism has been proposed in which reaction occurs from hydrogen atoms that are paired on the dimer prior to desorption, leading to a first-order rate law consistent with experimental measurements. The interaction between dangling bond orbital electrons (π bond) of the dimer pair has been identified as the driving force for pairing.⁴⁷ The silicon dimer, however, is not part of the Si(111)-(7 \times 7) structure, and if some feature *unique* to the dimer were responsible for the observed rovibrational distribution on this surface, we would not expect the same distribution from the Si(111)-(7 \times 7) surface.

We are thus led to a model in which the transition state for recombinative desorption is localized over a *single silicon atom*. The idea is as follows. If the reaction complex is strongly associated with one Si atom and interacts only weakly with adjacent surface atoms, then the largest contribution to the rovibrational distribution will be caused by potentials near a single silicon atom. As a result, the dynamics and resulting product state distribution might be largely insensitive to surface structure.

The idea of a reaction occurring at a single surface atom, which we propose here to explain the structure insensitivity in recombinative desorption dynamics, was put forth years ago as an explanation for structure insensitivity in catalysis. The role of surface structure in heterogeneous chemical reactions has been of interest for many years, with reactions often categorized as "structure sensitive" or "structure insensitive."^{2,18} A structure-insensitive reaction is one that is insensitive to details of the catalyst such as particle size or crystallographic plane of a single crystal. A structure-sensitive reaction, on the other hand, has a reactivity that can be strongly dependent upon catalyst preparation and structure. The degree of sensitivity of a catalytic reaction to surface structure has been interpreted in terms of the number of surface sites necessary in the rate-determining step (RDS) of the reaction, also referred to as ensemble size.⁶⁸ In 1976, Boudart⁶⁹ proposed that if the rate-determining step of a reaction requires only one surface atom, the reaction may change very little with surface geometry, whereas if the RDS requires several adjacent surface atoms, the reaction may be strongly surface sensitive.

We illustrate the single-site model for desorption occurring at a silicon dimer on the Si(100)-(2 \times 1) surface in Fig. 6(a). The reactants are a pair of hydrogen atoms on a single dimer, as discussed earlier, although reaction proceeds via a three-center transition state near only one of the Si atoms. This reaction could occur by H-atom migration across the dimer followed by H₂ formation and desorption occurring near a single Si atom. The possibility of a 1,2-hydrogen shift followed by 1,1-elimination, using molecular terminology, was also raised by Nachtigall *et al.*⁶⁰ based on their theoretical results. An illustration of the single-site desorption mechanism on the Si(111)-(7 \times 7) surface is given in Fig. 6(b). Here the reaction is shown occurring between hydrogen atoms from uncorrelated sites, consistent with second-order kinetics. Again, the transition state for recombinative

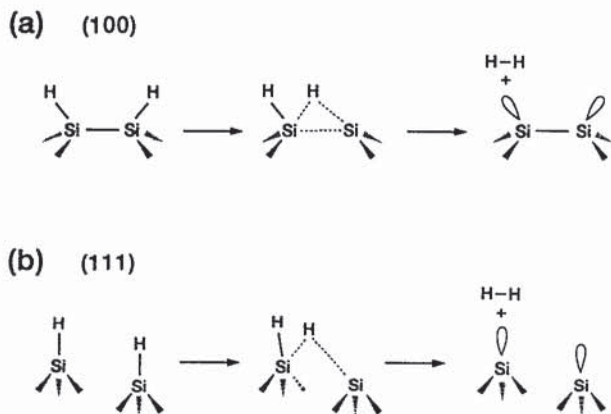
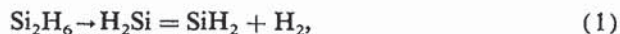


FIG. 6. Pictorial model of reaction pathway involved in the recombinative desorption of hydrogen from (a) Si(100)-(2×1) and (b) Si(111)-(7×7).

desorption is three center. We show the migrated H atom as forming a partial bond with the new silicon atom while retaining some interaction with its original silicon atom site. Based on the present results, we cannot distinguish whether the H-atom transfer involves complete scission of a Si–Si bond (i.e., with the formation of an actual dihydride species) or, at the other extreme, a completely pentavalent transition state. However, recent measurements of internal state distributions for hydrogen desorbed from the dihydride species²³ suggest that hydrogen desorption from the monohydride state occurs via a dihydride formed in a preequilibrium reaction.

Further support outside that of our present study exists for the proposed transition state configuration. The Si–Si spacing on the Si(100)-(2×1) surface dimer is large (2.4 Å), and delocalized bonding over the entire structure, as would exist for a symmetric, four-center transition state, might have a large energetic barrier. On the Si(111)-(7×7) surface, the Si–Si spacing is even larger (3.9 Å for the “1×1” rearrangement), and a four-center transition state physically seems even less likely to be energetically favorable on this surface. Furthermore, a symmetric, four-center transition state is symmetry forbidden for the analogous molecular reaction of H₂ addition to silylene (Si₂H₄).⁷⁰ Although the Woodward–Hoffmann rules may not be strictly applicable to surface reactions, a large barrier for the symmetric pathway might be expected.

Calculations performed on the 1,2-elimination reaction of disilane,



also support this mechanism. Reaction (1) is the molecular analog to the recombinative desorption of H₂ from the dimer site on the Si(100)-(2×1) surface. Gordon, Truong, and Bonderson⁷¹ and Ho *et al.*⁷² have performed *ab initio* calculations on this system and found that although less endothermic, the 1,2-elimination has a much higher activation barrier than the alternate 1,1-elimination (which is somewhat analogous to dihydride desorption). Upon further investigation of the 1,2-elimination reaction pathway, Gordon, Truong, and Bonderson⁷¹ found that at the transition state, both

reacting hydrogens are closer to one of the silicon atoms, resembling a silane-silylene complex, H₄Si–SiH₂, following migration of one hydrogen atom. Agrawal, Thompson, and Raff⁷³ applied classical trajectory methods to study this system; they also concluded that the 1,2-elimination reaction proceeds by rupture of one Si–H bond and transfer of this atom to the other hydrogen, followed by a reaction resembling hydrogen-atom abstraction. The *d* orbitals of silicon appear to play an important role in stabilizing the silane-silylene intermediate; Gordon *et al.*⁷¹ note that without the addition of *d* orbitals to silicon, the reacting hydrogens are predicted to be between the two silicon atoms.

B. Comparison of kinetics and dynamics

At first it might seem anomalous that we observe the same rovibrational distribution for desorbed H₂ on both the Si(100)-(2×1) and Si(111)-(7×7) surfaces, despite the fact that the kinetics are characterized by different reaction orders. This prompts us to consider how surface structure might influence either kinetics or dynamics. In general, a state-resolved experiment might be expected to yield more detailed information than a kinetics experiment, which measures an average phenomenon and, therefore, the dynamical study would reveal even greater differences between the two surfaces. Such a prediction, however, is based on the notion that both experiments involve the same quantities, which is in fact not the case. Both types of studies measure different features of the recombinative desorption process.

Let us consider the kinetic rate expression in the Arrhenius form:

$$\text{Reaction rate} = A \times e^{(-E_{\text{act}}/RT)} \times [A]^m \times [B]^n \dots,$$

where *A* is the preexponential, or frequency, factor for the reaction, *E*_{act} is the activation energy, *R* is the gas constant, *T* is the absolute temperature, and *m* and *n* are the reaction order with respect to reactants *A* and *B*, respectively. Almost all rate laws can be written in this empirical form. A look at the origin of these terms as described by collision theory is instructive. In collision theory, the rate of a chemical reaction is proportional to the probability of collision, *Z*, between reactants (*Z* ∝ [*A*]^{*m*} × [*B*]^{*n*}); the fraction that has sufficient energy to react (*e*^{−*E*_{act}/*RT*}); and a steric or entropic term that indicates the orientational restrictions on reaction (*A* = *e*^{Δ*S*′/*R*}).⁷⁴

The reaction order is a measure of the concentration dependence of the frequency with which the reactants will collide. This is a transport property⁷⁴ that does not describe what occurs beyond the collision. Let us consider the reaction order measured for the H₂/Si system. The observation of a first-order rate for recombinative desorption on the Si(100)-(2×1) surface indicates that the probability of collision is proportional to the concentration of only one of the reactant atoms. Sinniah *et al.*¹⁶ first proposed a two-step model for the process, in which an *irreversible* excitation of one hydrogen atom into a freely translating state is followed by a faster recombination step with a normally bound hydrogen atom. The probability of reaction is then proportional to the probability of the first excitation step occurring, or [*H*].

A second model was proposed¹³ (and appears to be gaining wider acceptance^{17,34,47,59,61}), in which reaction occurs between two H atoms that have previously paired at some site. Several groups have suggested that the hydrogen atoms are paired on the same silicon dimer on the Si(100)-(2×1) surface, as illustrated in Fig. 6(a).^{13,17,34,47,61} Wu and Carter⁵⁹ have proposed a prepairing of two H atoms on adjacent silicon dimers in the same row. The kinetics of a pairing mechanism are first order,

$$\text{rate} = k \times [\text{H-H}_{\text{pair}}] = k' \times [\text{H}],$$

since $[\text{H-H}_{\text{pair}}] = [\text{H}] \times \frac{1}{2}$ in the limit of complete pairing. In actuality, the pairing must be treated as an equilibrium process under some driving force.^{17,61} The driving force for pairing on a single dimer has been identified as the π -bonding interaction between the dangling bond orbitals, which is lost each time an H atom adsorbs onto an unoccupied dimer.

On the Si(111)-(7×7) surface, upon which the reaction is second order at higher coverages and intermediate between first and second order at lower coverages, Reider *et al.*²⁰ have proposed a model that involves at least two distinct adsorption sites, each with a different binding energy and propensity for reaction. Their model can reproduce the observed variation of kinetic order with coverage on the Si(111)-(7×7) surface.

All of these models address the probability of encounter. A dynamics measurement, however, is sensitive not to how the reactants find each other on the surface, but rather to how they traverse the transition-state region once they have entered into a reactive encounter. It is not the reaction order, but the preexponential factor and the activation energy that are sensitive to details about the transition state. Thus we might expect that a comparison of these values measured on the two surfaces would be more revealing as to the dynamics.

Several groups have reported activation energies and preexponential factors for desorption of H₂ from the Si(100) and Si(111) surfaces. Unfortunately, despite close agreement between actual desorption rate, most of the published kinetic parameters on a given surface vary significantly, and thus comparisons between the two surfaces are difficult to make. Reported activation energies range from as low as 45 kcal/mol (Refs. 16 and 25) to ~60 kcal/mol, (Refs. 5, 13, 15, 17, and 20) and preexponential factors from ~10¹¹ s⁻¹ (Ref. 16) to 10¹⁷ s⁻¹ (Ref. 13) on the (100) surface and 0.05 cm² s⁻¹ to ~200 cm² s⁻¹ on the (111) surface (Refs. 5, 13, 15, 20, and 25). Only two groups have measured kinetic data from both surfaces with the same apparatus. Wise *et al.*¹³ report $E_{\text{act}} = 58 \pm 2$ kcal/mol and $A = (5.5 \pm 0.5) \times 10^{15}$ s⁻¹ for first-order desorption from Si(100)-(2×1) and $E_{\text{act}} = 62 \pm 4$ kcal/mol and $A = 91 \pm 10$ cm² s⁻¹ for second-order desorption from Si(111)-(7×7) by laser-induced thermal desorption measurements. These values are notably similar (considering that the pseudo-first-order prefactor is 7.2×10^{16} on Si(111), using $\theta_{\text{sat}} = 7.93 \times 10^{14}$ cm⁻²)⁵. Heinz and co-workers^{17,20} also measure $E_{\text{act}} = 56$ –58 kcal/mol on both surfaces.

Although agreement is not complete, most of the measured values for activation energy are close to 60 kcal/mol on both surfaces.^{5,13,15,20} The same activation barrier would

indicate that the energetic expense necessary to reach the transition state is similar on both surfaces, and suggests a relationship between the reaction complex on the (111) and (100) surfaces. As discussed in Sec. IV A, we have proposed, based on the similarities in the product rovibrational distribution, that the transition state is related on the two surfaces. This relation does not in itself imply that the energy required to reach the transition state is the same, because although the local environment of the hydrogen atoms at the transition state (to which our measurement is sensitive) might be similar, the remaining Si surface structure is not, as evident in Fig. 6. We find the apparent agreement in activation energy between the (100) and (111) surfaces significant.

A relationship might be expected between the preexponential factor and the rotational distribution, because both observables are controlled by similar dynamical features of the reaction. The preexponential factor is an entropic term that indicates the steric requirements for reaction, including details about orientation and how close the reactants must approach one another (i.e., the impact parameter).⁷⁴ The product rotational distribution is influenced by the same factors. In reaction dynamics, the rotational distribution of the products may even be directly related, in certain cases, to the impact parameter of collision or to the specific orientation of reactants at the transition state.⁷⁵

In these studies of H₂ desorption from Si, we find that the average rotational energy of the desorbed H₂ is low, indicating that recombination occurs through a transition state that is oriented symmetrically relative to the hypersurface corrugation. A highly constrained geometry in the transition state, such as the one described here, is usually associated with a low value of the Arrhenius preexponential factor. Normal preexponential factors for a recombinative desorption reaction fall into the range of 10¹¹–10¹⁹ s⁻¹,⁷⁶ wherein the low values are usually associated with an immobile activated complex and the high values with an activated complex having rotational and translational degrees of freedom. However, of all the reported values for this reaction, only Sinniah *et al.*¹⁶ have measured a low preexponential factor. As discussed earlier, it might be appropriate to compare the recombinative desorption of hydrogen from silicon with intramolecular gas-phase elimination reactions. These reactions generally have preexponential factors near 10¹³ s⁻¹.⁷⁷ In any case, an accurate interpretation of the preexponential factor for H₂ desorption from Si will be difficult until a definitive value is agreed upon in the literature.

In summary, we believe that the similarity of rovibrational distributions is not in contradiction with the different kinetic order on the (100)-(2×1) and (111)-(7×7) surfaces of silicon. Understanding which features of the reaction are probed by each type of measurement is important. Whereas the kinetic order is related to the probability of getting the reactants together, the dynamics describe what happens as the reactions occurs.

C. Implications for other covalent systems

Recently, kinetic measurements of H₂ desorption have been reported for β -silicon carbide,⁷⁸ diamond,⁷⁹ germani-

um,^{80,81} gallium arsenide,⁸² and tellurium⁸³ surfaces. These other covalent materials are interesting to compare with the H₂/Si system. In these systems, as for silicon, molecular hydrogen does not react with the surface, whereas atomic hydrogen reacts readily. This property is in contrast with most metallic surfaces, upon which molecular hydrogen will dissociatively adsorb (exceptions are the coinage metals—Au, Ag, and Cu).

One interesting similarity is that on the (100) crystallographic face of the Si, Ge, and diamond surfaces, the recombinative desorption of hydrogen follows a first-order rate law. A general feature on each of these surfaces is the presence of dimers, suggesting that the dimers play an important role in the overall desorption mechanism.⁶¹ First-order kinetics were also observed for desorption of H₂ from polycrystalline Te and from polycrystalline β-SiC. Unusual kinetic rate orders appear characteristic of covalent solids, and conventional models of recombinative desorption that accurately predict behavior on metal surfaces are not adequate on these covalent surfaces.

The influence of surface structure on the dynamics of hydrogen recombinative desorption from silicon surfaces contrasts with that from metal surfaces. Although the present state-specific study reveals no significant difference in rovibrational distribution between the Si(100) and Si(111) surfaces, structural effects on recombination dynamics have been observed for the H₂/metal systems. In their state-specific studies of H₂ recombinative desorption from both the Cu(110) and Cu(111) surfaces, Kubiak *et al.*⁶² observed that the amount of vibrational excitation differed by a factor of 2 between the two surfaces, whereas the rotational distribution was unchanged. Studies of the recombinative desorption of H₂ from Cu (Ref. 62) [and also of N₂ from Fe (Ref. 84)] have shown that modification of the surface electronic structure by coadsorption of sulfur dramatically affects the vibrational distribution.

Although state-specific studies of hydrogen desorption have not been performed to date on any other covalent systems, the internal state distribution of hydrogen desorbed from such surfaces might, by analogy to the silicon surface, exhibit little structure sensitivity. We suggest that the detailed dynamical description presented here should be applicable to other covalent systems. In each of these systems, the interaction of hydrogen with the surface is strong and highly directional. Allendorf and Outka⁷⁸ have suggested from their work on β-SiC that hydrogen desorption from that surface involves loss of molecular hydrogen from a single surface silicon atom. Outka⁸³ has proposed that hydrogen desorption from tellurium has a special site requirement. These interpretations are in agreement with the picture presented here—that of a local model for recombinative desorption of hydrogen that involves a transition state localized at a single silicon atom.

ACKNOWLEDGMENTS

S.F.S. gratefully acknowledges a graduate fellowship from the National Science Foundation and a grant from AT&T Bell Laboratories. K.W.K. acknowledges support from the Procter & Gamble Foundation and Phi Beta Kappa

of Northern California. We thank J. Zhang, T. Heinz, H. Zacharias, and M. D'Evelyn for making their results available to us prior to publication. This project is supported by the Office of Naval Research under Grant No. N00014-91-J1023.

¹R. Hoffmann, *Solids and Surfaces: A Chemist's View of Bonding in Extended Structures* (VCH Publishers, New York, 1988).

²A. Zangwill, *Physics at Surfaces* (Cambridge University Press, New York, 1988).

³J. J. Boland, *Surf. Sci.* **244**, 1 (1991).

⁴R. Imbihl, J. E. Demuth, S. M. Gates, and B. A. Scott, *Phys. Rev. B* **39**, 5222 (1989).

⁵G. Schulze and M. Henzler, *Surf. Sci.* **124**, 336 (1983).

⁶H. Froitzheim, U. Köhler, and H. Lammering, *Surf. Sci.* **149**, 537 (1985).

⁷S. Ciraci, R. Butz, E. M. Oellig, and H. Wagner, *Phys. Rev. B* **30**, 711 (1984).

⁸U. Jansson and K. Uram, *J. Chem. Phys.* **91**, 7978 (1989).

⁹J. J. Boland, *J. Phys. Chem.* **95**, 1521 (1991).

¹⁰For a review of the atomic and electronic structure of clean and adsorbate-covered silicon surfaces, including hydrogen, see R. I. G. Uhrberg and G. V. Hansson, *Crit. Rev. Solid State Mater. Sci.* **17**, 133 (1991).

¹¹B. I. Craig and P. V. Smith, *Surf. Sci.* **226**, L55 (1990).

¹²S. M. Gates, R. Kunz, and C. M. Greenlief, *Surf. Sci.* **207**, 364 (1989).

¹³M. L. Wise, B. G. Koehler, P. Gupta, P. A. Coon, and S. M. George, *Surf. Sci.* **258**, 166 (1991).

¹⁴C. C. Cheng and J. T. Yates, Jr., *Phys. Rev. B* **43**, 4041 (1991).

¹⁵B. G. Koehler, C. H. Mak, D. A. Arthur, P. A. Coon, and S. M. George, *J. Chem. Phys.* **89**, 1709 (1988).

¹⁶K. Sinniah, M. G. Sherman, L. B. Lewis, W. H. Weinberg, J. T. Yates, Jr., and K. C. Janda, *J. Chem. Phys.* **92**, 5700 (1990).

¹⁷U. Höfer, L. Li, and T. F. Heinz, *Phys. Rev. B* **45**, 9485 (1992).

¹⁸M. Boudart and G. Djega-Mariadassou, *Kinetics of Heterogeneous Catalytic Reactions* (Princeton University Press, Princeton, 1984).

¹⁹K. Christmann, *Surf. Sci. Rep.* **9**, 1 (1988).

²⁰G. A. Reider, U. Höfer, and T. F. Heinz, *J. Chem. Phys.* **94**, 4080 (1991).

²¹G. A. Reider, U. Höfer, and T. F. Heinz, *Phys. Rev. Lett.* **66**, 1994 (1991).

²²Note that structure refers to both electronic and geometric structure of the surface. M. Boudart, in *Proceedings of the Welch Foundation Conferences on Chemical Research*, edited by W. O. Milligan (Robert A. Welch Foundation, Houston, Texas, 1970), pp. 299; M. Boudart, *J. Am. Chem. Soc.* **72**, 1040 (1950).

²³S. F. Shane, K. W. Kolasinski, and R. N. Zare, *J. Chem. Phys.* (to be published).

²⁴J. T. Law, *J. Phys. Chem.* **30**, 1568 (1959).

²⁵Y. I. Belyakov, N. I. Ionov, and T. N. Kompaniets, *Sov. Phys. Solid State* **14**, 2567 (1973).

²⁶M. I. Datsiev and Y. I. Belyakov, *Sov. Phys. Tech. Phys.* **15**, 166 (1970).

²⁷M. Liehr, C. M. Greenlief, M. Offenberger, and S. R. Kasi, *J. Vac. Sci. Technol. A* **8**, 2960 (1990).

²⁸S. M. Gates, *Surf. Sci.* **195**, 307 (1988).

²⁹C. M. Greenlief, S. M. Gates, and P. A. Holbert, *J. Vac. Sci. Technol. A* **7**, 1845 (1989).

³⁰F. Bozso and P. Avouris, *Phys. Rev. B* **38**, 3943 (1988).

³¹K. J. Uram and U. Jansson, *J. Vac. Sci. Technol. B* **7**, 1176 (1989).

³²S. F. Shane, K. W. Kolasinski, and R. N. Zare, *J. Vac. Sci. Technol. A* (to be published).

³³J. A. Appelbaum and D. R. Hamann, in *Topics in Current Physics: Theory of Chemisorption*, edited by J. R. Smith (Springer-Verlag, Berlin, 1980).

³⁴K. W. Kolasinski, S. F. Shane, and R. N. Zare, *J. Chem. Phys.* **96**, 3995 (1992).

³⁵K.-D. Rinnen, M. A. Buntine, D. A. V. Kliner, R. N. Zare, and W. M. Huo, *J. Chem. Phys.* **95**, 214 (1991).

³⁶S. Speiser and J. Jortner, *Chem. Phys. Lett.* **44**, 399 (1976).

³⁷R. G. Bray and R. M. Hochstrasser, *Mol. Phys.* **31**, 1199 (1976).

³⁸J. Xie, Ph.D. thesis, Stanford University, 1991.

³⁹Y. J. Chabal, G. S. Higashi, and S. B. Christman, *Phys. Rev. B* **28**, 4472 (1983).

⁴⁰K. C. Pandey, T. Sakurai, and H. D. Hagstrum, *Phys. Rev. Lett.* **35**, 1729 (1975).

⁴¹The rotational distribution for H₂(*v* = 1) desorbed from Si(111) was measured only once. Because of low signal levels, the surface was dosed

- with atomic hydrogen. In previous studies, the source of surface hydrogen was found to have no effect on the rovibrational distribution of the desorbed H₂ (Ref. 32).
- ⁴²L. Schröter, Ch. Trame, R. David, and H. Zacharias (unpublished).
- ⁴³J. M. Jasinski and S. M. Gates, *Acct. Chem. Res.* **24**, 9 (1991).
- ⁴⁴F. Bozso and P. Avouris, *Phys. Rev. B* **38**, 3943 (1989).
- ⁴⁵Y. Suda, D. Lubben, T. Motooka, and J. E. Greene, *J. Vac. Sci. Technol. B* **7**, 1171 (1989).
- ⁴⁶J. Uram and U. Jansson, *Surf. Sci.* **249**, 105 (1991).
- ⁴⁷J. J. Boland, *Phys. Rev. Lett.* **67**, 1539 (1991).
- ⁴⁸J. J. Boland, *Phys. Rev. B* **44**, 1383 (1991).
- ⁴⁹J. J. Boland, *Phys. Rev. Lett.* **65**, 3325 (1990).
- ⁵⁰K. W. Kolasinski, Ph.D. thesis, Stanford University, 1992.
- ⁵¹G. E. Busch and K. R. Wilson, *J. Chem. Phys.* **56**, 3626 (1972).
- ⁵²R. Bersohn, *J. Phys. Chem.* **88**, 5145 (1984).
- ⁵³N. H. Hijazi and J. C. Polanyi, *Chem. Phys.* **11**, 1 (1975).
- ⁵⁴E. Hasselbrink, *Chem. Phys. Lett.* **170**, 329 (1990).
- ⁵⁵J. Sheng and J. Z. H. Zhang, *J. Chem. Phys.* (to be published).
- ⁵⁶R. I. G. Uhrberg and G. V. Hansson, *Crit. Rev. Solid State Mater. Sci.* **17**, 133 (1991).
- ⁵⁷J. A. Appelbaum, G. A. Baraff, and D. R. Hamann, *Phys. Rev. B* **14**, 588 (1976).
- ⁵⁸A. Redondo and W. A. Goddard III, *J. Vac. Sci. Technol.* **21**, 344 (1982).
- ⁵⁹C. J. Wu and E. A. Carter, *Chem. Phys. Lett.* **185**, 172 (1991).
- ⁶⁰P. Nachtigall, K. D. Jordan, and K. C. Janda, *J. Chem. Phys.* **95**, 8652 (1991).
- ⁶¹M. P. D'Evelyn, Y. L. Yang, and L. F. Sutcu, *J. Chem. Phys.* **96**, 852 (1992).
- ⁶²G. D. Kubiak, G. O. Sitz, and R. N. Zare, *J. Chem. Phys.* **83**, 2538 (1985).
- ⁶³R. M. Tromp, R. J. Hamers, and J. E. Demuth, *Phys. Rev. Lett.* **55**, 1303 (1985).
- ⁶⁴R. Wolkow, *Phys. Rev. Lett.* **68**, 2636 (1992).
- ⁶⁵A general two-site model, under which the specific case of a defect model falls, is discussed in Ref. 20.
- ⁶⁶S. F. Shane (unpublished).
- ⁶⁷P. Gupta, V. L. Colvin, and S. M. George, *Phys. Rev. B* **37**, 8234 (1988).
- ⁶⁸W. M. H. Sachtler, *Disc. Faraday Soc.* **72**, 7 (1981).
- ⁶⁹M. Boudart, in *Proceedings of the 6th International Congress on Catalysis*, edited by G. C. Bond, P. B. Wells, and F. C. Tompkins (The Chemical Society, London, 1976), p. 90.
- ⁷⁰R. B. Woodward and R. Hoffman, *The Conservation of Orbital Symmetry* (Verlag Chemie, Weinheim, 1969).
- ⁷¹M. S. Gordon, T. N. Truong, and E. K. Bonderson, *J. Am. Chem. Soc.* **108**, 1421 (1986).
- ⁷²P. Ho, M. E. Coltrin, J. S. Binkley, and C. F. Melius, *J. Phys. Chem.* **90**, 3399 (1986).
- ⁷³P. M. Agrawal, D. L. Thompson, and L. M. Raff, *J. Chem. Phys.* **92**, 1069 (1990).
- ⁷⁴P. W. Atkins, *Physical Chemistry* (Freeman, New York, 1986).
- ⁷⁵R. D. Levine and R. B. Bernstein, *Molecular Reaction Dynamics and Chemical Reactivity* (Oxford University Press, New York, 1987).
- ⁷⁶V. P. Zhdanov, *Surf. Sci. Rep.* **12**, 183 (1991).
- ⁷⁷S. W. Benson, *Thermochemical Kinetics* (Wiley, New York, 1968).
- ⁷⁸M. D. Allendorf and D. A. Outka, *Surf. Sci.* **258**, 177 (1991).
- ⁷⁹A. V. Hamza, G. D. Kubiak, and R. H. Stulen, *Surf. Sci.* **237**, 35 (1990).
- ⁸⁰J. E. Crowell (private communication).
- ⁸¹M. D'Evelyn (private communication).
- ⁸²J. R. Creighton, *J. Vac. Sci. Technol. A* **8**, 3984 (1990); W. Mokwa, D. Kohl, and G. Heiland, *Phys. Rev. B* **29**, 6709 (1984).
- ⁸³D. A. Outka, *Surf. Sci.* **235**, L311 (1990).
- ⁸⁴R. P. Thorman and S. L. Bernasek, *J. Chem. Phys.* **74**, 6498 (1981).
- ⁸⁵K. Takayanagi, Y. Tanishiro, M. Takahashi, and S. Takahashi, *J. Vac. Sci. Technol. A* **3**, 1502 (1985).